Supplementary Information

Materials and Methods

Isolation and sorting of OBs

OBs were isolated from the femurs of 3-month-old and 18-month-old mice. After flushing out the bone marrow with PBS, the bone tissue was cut into small pieces. These bone fragments were then digested overnight at 37°C using Type II collagenase and subsequently cultured in α-MEM supplemented with 10% FBS. A few days later, adherent OBs were collected by removing the bone fragments. For td-Tomato reporter mice, OBs were processed as described and subsequently sorted using flow cytometry.

Culture and osteogenic induction of 3T3-E1 cells

MC3T3-E1 cells are grown in Dulbecco's Modified Eagle's Medium (DMEM, Gibco) medium (GM) supplemented with 10% FBS (Gibco), 10 mM HEPES (Sigma), 63 mg/L penicillin (Sigma), and 100 mg/L streptomycin (Sigma). The cells are maintained in a humidified incubator at 37°C with an atmosphere of 5% CO_2. For osteogenic differentiation, the cells are induced with an osteogenic induction medium (OM), which consists of 10% FBS in DMEM, 50 μM ascorbic acid, 10 mM β-glycerol phosphate, and 100 nM dexamethasone.

Western blot

For the extraction of total proteins from OBs, cells were lysed in RIPA buffer supplemented with a phosphatase and protease inhibitor cocktail (PIC, HY-K0010, MedChemExpress). For bone tissues, femurs were isolated from soft tissues, and the mid-shaft portions were ground into a fine powder under liquid nitrogen. These powders were then lysed in RIPA buffer containing the same inhibitor cocktail for 30 minutes at 4°C. After centrifugation at 12,000 rpm, the supernatant was collected, and the proteins were denatured and separated by SDS-PAGE. The resolved proteins were transferred onto PVDF membranes, which were then probed with specific primary antibodies, including anti-P16 (1:1000, 30519-1-AP, Proteintech), anti-H2AK119ub1 (1:1000, 8240S, Cell Signaling Technology), anti-KDM2B (1:1000) , anti-PCGF1 (1:1000) (*1, 2*), anti-RING1B (Abcam, ab254343, 1:1000), anti-β-Catenin (1:1000, 9562S, Cell signaling Technology), anti-BCOR (1:1000, 30519-1-AP, Proteintech), anti-TUBULIN (1:5000, A17910, ABclonal), anti-GAPDH (1:5000, A19056**,** ABclonal), anti-H3 (1:5000, 9715S, Cell Signaling Technology). Following incubation with appropriate secondary antibodies, the blots were visualized using the NcmECL High Reagent (P2300, New Cell & Molecular Biotech) and captured with a Uvitec Cambridge Imaging System. The protein bands were quantified by normalizing to an internal control.

RNA sequencing

RNA sequencing was conducted by Novogene, using an Illumina Novaseq platform to generate 150 bp paired-end reads. Clean reads were aligned to the mm39 reference genome with Hisat2 (v2.2.1), and Samtools (v1.19) was used to convert sam files to bam files. Deeptools (v3.5.4) was employed to generate bigwig files, with visualization done via Integrative Genomics Viewer. Gene counts were calculated by Stringtie (v2.2.1), and differential expression analysis was performed using the R package

DESeq2 (v1.34.0). Genes were considered significantly different if they met the criteria of p-value < 0.05 and |log2FoldChange| > 0.585. Volcano plots and heatmaps were generated with R packages ggplot2 (v3.4.3) and pheatmap (v1.0.12). FPKM values were extracted using R packages Ballgown (v2.26.0). Pathway enrichment analysis was performed using Metascape, and selected pathways were visualized with R packages ggplot2 (v3.4.3)(*3*).

CUT&Tag

The CUT&Tag assay was performed using the Hyperactive Universal CUT&Tag Assay Kit (TD904, Vazyme) as previously described (*4*). Briefly, 100,000 cells were harvested, washed, and resuspended in wash buffer before incubation with pre-activated conconavalin A beads. Primary anti-H2AK119ub1 (1:1000, 8240S, Cell Signaling Technology) antibody and secondary antibodies were added sequentially, followed by incubation with Dig-wash buffer and pA/G-Tnp Pro. After DNA extraction and PCR amplification, sequencing was performed on an Illumina Novaseq6000 platform (Annoroad Gene Technology, Beijing). Raw data underwent quality evaluation with Fastqc (v0.12.1) and Multiqc (v1.19). Adapters were removed with Trim-galore (v0.6.10). Clean reads were aligned to the mm39 reference genome and λDNA (TD904, Vazyme), normalized based on scale-factor, and duplicates removed with Sambamba (v1.0). Peak calling was conducted with Macs2 (v2.2.9.1), and bigwig files were generated with Deeptools (v3.5.4). Peaks were annotated with R packages ChIPseeker (v1.30.3), and pathway enrichment analysis was performed using Metascape. (https://metascape.org/gp/index.html). Visualization of selected pathway were generated by R packages ggplot2(v3.4.3) (*3*).

μCT

To observe and evaluate bone microstructure, μCT analysis was performed. Briefly, femurs were harvested from mice, fixed overnight in 4% paraformaldehyde, and scanned with an isotropic voxel size of 8 μm and a peak tube voltage of 55 kV and current of 100 μA (SKYSCAN 1276; Bruker). Three-dimensional images were reconstructed and regions of interest (ROI) were analyzed using NReconServer, CTAn, and CTvox softwares (GE). Trabecular bone parameters were measured from 100 consecutive slices of the distal metaphysis, devoid of epiphyseal structures.

Calcein double labeling and three-point bending test

For calcein double labeling, mice were injected with calcein at 10 mg/kg on day 13 and day 3 prior to femur harvest. Femurs were fixed, embedded in methylmethacrylate, and sectioned at 5μm. Images were acquired using a fluorescence confocal microscope, and bone formation rates (BFR/BS and BFR/TV) were calculated from fluorochrome double labels at periosteal and endocortical surfaces using OsteoMeasure software. The three-point bending test was conducted on fresh femurs to assess structural and material strength using an Instron electromechanical tester (Instron 3367). Load-displacement curves were recorded until fracture, and the maximum force at failure was calculated.

H&E staining, TRAP staining and IHC

Samples including femurs, heart, liver, spleen, lung, and kidney were collected and sectioned at 5 μm for H&E staining. Paraffin sections were dewaxed, stained with hematoxylin and eosin, dehydrated, and sealed (*5*). For IHC, slides were stained with

specific antibodies: anti-WNT2 (1:100, 66656-1-Ig, Proteintech), anti-WNT3a (1:100, 26744-1-AP, Proteintech), anti-β-Catenin (1:100, 9562S, Cell signaling Technology) antibody. Sections were deparaffinized, rehydrated, and antigen retrieval was performed with 3% hydrogen peroxide. After blocking with 3% BSA, primary and secondary antibodies were applied, and DAB substrate was used to develop signals. For TRAP staining, sections were deparaffinized, rehydrated, and stained with a TRAP staining kit (G1050, Servicebio). Images were scanned at ×100 magnification (Pannoramic 250 FLASH, 3DHISTECH), and OB/OC counts were performed using ImageJ software.

IF staining

Femurs were fixed in 4% paraformaldehyde and decalcified in EDTA solution before embedding in OCT compound and sectioning at 8 μm. Sections were stained with an anti-β-Catenin antibody. For OBs, cells were fixed, permeated, and incubated with primary antibodies: RUNX2 (1:100, 12556S, Cell Signaling Technology), ALP (1:100, AB_2838191, Affinity Biosciences Cat# DF6225) and secondary antibodies before image capture with a fluorescence microscope.

ChIP-PCR analysis

Cells (1×10^6) were used for each immunoprecipitation following a previously described protocol (*4*). In brief, cells were crosslinked with 1% formaldehyde at room temperature (RT) in medium for 10 min, after which glycine was added to a final concentration of 0.125 M to quench the crosslinking and incubate at room temperature for 5 min. Cells were washed twice with PBS and lysed with SDS buffer (100 mM NaCl, 50 mM pH 8.1 Tris-HCl, 5 mM pH 8.0 EDTA, 0.02% NaN_3, 0.5% SDS, PIC) at RT for 5min. Cell lysates were harvested, and samples were thawed in a water bath to ensure complete dissolution of SDS. After centrifugation at 4 ℃ 1200 rpm for 6 min, the supernatant was discarded and 1 mL of prechilled IP buffer (a mixture of SDS buffer and Triton Dilution Buffer in a 2:1 ratio, supplemented with PIC) was added. Samples were then sonicated to produce 0.2-0.5 Kb DNA fragments, centrifuge sonicated chromatin 13,000 rpm for 30 min.

Equal amount of protein was taken, and the volume was adjusted to 1 mL with IP buffer. Primary antibodies, including anti-β-Catenin (5 μg, 9562S, Cell Signaling Technology), anti-H2AK119ub1 (1:1000, 8240S, Cell Signaling Technology), anti-PCGF1 (5 μg), anti-RING1B (5 μg, 5694S, Cell Signaling Technology), or normal IgG, were added for immunoprecipitation overnight at 4°C with rotation. Protein A/G beads were then added and incubated on a rotating wheel at 4℃ for 2 hrs. Beads were washed once with 1 mL of 150 mM wash buffer (containing 1% TritonX-100, 0.1% SDS, 150 mM NaCl, 2 mM EDTA pH 8.0, 20 mM Tris-HCl pH 8.0), and then twice with 500 mM wash buffer (containing 1% TritonX-100, 0.1% SDS, 500 mM NaCl, 2 mM EDTA pH 8.0, 20 mM Tris-HCl pH 8.0). Finally, 120 μL of de-crosslinking buffer was added to both input and IP samples and incubated at 65°C overnight at 1200 rpm to elute the complexes from the beads. QIAGEN PCR purification kit was used for ChIP-DNA purification, and the samples were quantified by real-time PCR using primers listed in data file S5.

RNA isolation and qRT-PCR

Total RNA was isolated using kit (M050, New Cell & Molecular Biotech) and reverse

transcribed using HiScript III All-in-one RT SuperMix (R333-01, Vazyme). qRT-PCR was conducted using SYBR Green Master Mix (Q711-03, Vazyme). Real-time quantitative PCR was performed with the LightCycler480 system. The relative expression of target genes was calculated using method of $2^{-\Delta\Delta CT}$. Primers used in qRT-PCR was listed in data file S5.

Dual luciferase assay

To detect relative luciferase activity of TOP reporter, 3T3-E1 cells were co-transfected with 100 ng TOP-FLASH plasmid harboring six TCF-binding motifs (Millipore), and 2 ng of the renilla luciferase control vector pGL4.74 (Promega). Following a 7-day incubation in osteogenic induction medium, cell lysates were prepared using the lysis buffer from the TransDetect® Double-Luciferase Reporter Assay Kit (FR201, TransGen Biotech, China). Luciferase activity was subsequently quantified using a GloMax 20/20 luminometer (Promega).

Stability Assay of iBP

The stability of iBP (400 μM) was assessed using HPLC following incubation in cell culture media (DMEM) supplemented with 10% FBS at 37 °C for 0, 12, or 24 hrs. To facilitate the precipitation of proteins from FBS, the incubation mixture was diluted with a four-fold volume of acetonitrile and centrifuged. The resulting supernatant was then subjected to HPLC analysis to determine the remaining iBP concentration.

HPLC

HPLC analysis for iBP was conducted using a Shimadzu LC-20AT system equipped with an SPD-20A UV-VIS detector. The chromatographic separation was achieved on a 4.6 × 150 mm Agilent Eclipse XDB-C18 5 μm column. The mobile phase consisted of solvent A (water with 0.1% trifluoroacetic acid) and solvent B (acetonitrile) at a flow rate of 1.0 mL/min. The gradient elution program was as follows: 10% B (0−2 min), 10−100% B (2−16 min), 100% B (16−18 min), 100−80 % B (18−19 min) and 80% B (19−20 min).

Mouse PK Study

A standard pharmacokinetic study was conducted on iBP using C57BL/6J mice (n=3). The intraperitoneal injection formulation consisted of a 4 mg/mL solution of iBP prepared with a ratio of 10% DMSO, 40% PEG300, 5% Tween 80, and 45% Saline. The mice were administered iBP intraperitoneally at a dosage of 20 mg/kg, and plasma samples were collected at intervals of 5 min, 15 min, 30 min, 1 hr, 2 hrs, 4 hrs, 8 hrs, and 24 hrs post-injection. The harvested supernatant was diluted with water at a 1:2 ratio, and 2 μL of the diluted supernatant was subjected to LC/MS/MS for quantitative analysis.

High-throughput screening with AutoDock Vina

Compounds from ZINC database were subject to docking by using AutoDock Vina. Structure of $PCGF1^{RAWUL}$ was taken from crystal structure of $PCGF1^{RAWUL}$ – $BCOR^{PUFD}$ complex (PDB code 4HPL). pdbqt file of $PCGF1^{RAWUL}$ was generated usinig MGL Tools. $PCGF1^{RAWUL}$ protein was prepared by adding hydrogen atoms and Kolloman charges. The grid box was generated using grid-box option from MGL Tools. Each ligand was docked using exhaustiveness value of 16, and energy_range value of 0.1.

Protein purification

The cDNA encoding PCGF1^{RAWUL} L238A/F242A mutant (amino acids 166-255) was cloned into pGEX 6P-1 vector with N-terminal GST and hexa-histidine tag followed by PreScission Protease cleavage site. The cDNA encoding BCOR^{PUFD} (residues 1580-1696) was cloned into pET-28a vector with N-terminal hexa-histidine tag. Both PCGF1^{RAWUL} L238A/F242A mutant and BCOR^{PUFD} were expressed in *E. coli* BL21 (DE3) strain, respectively. Cultures were grown at 37 °C to OD_{600} of 0.6-0.8 before induction with 0.5 mM IPTG, and incubated for an additional 20 hrs at 16°C to promote protein expression.

For the purification of PCGF1^{RAWUL} L238A/F242A mutant, cells were harvested and resuspended in lysis buffer (20 mM Tris pH 8.0, 1 M NaCl, 7 mM β-mercaptoethanol, 5% glycerol). The recombinant protein was purified using Ni^{2+} affinity chromatography, followed by cleavage of the GST and His tags with PreScission Protease. The mutant PCGF1 ^{RAWUL} was further refined by additional Ni^{2+} affinity chromatography and gel filtration on a Superdex 75 (16/60) column pre-equilibrated with a buffer comprising 20 mM HEPES pH 7.5, 150 mM NaCl, 10% glycerol, and 0.5 mM TCEP. His-BCOR^{PUFD} was purified using a similar Ni^{2+} affinity chromatography approach, followed by gel filtration on a Superdex 75 (16/60) column.

AlphaScreen assay

The PCGF1^{RAWUL} L238A/F242A mutant was biotinylated using Biotinylation kit (G-MM-IGT, Genemore, Shanghai, China) according to manufacture's instructions. A concentration of 200 nM biotinylated PCGF1^{RAWUL} L238A/F242A mutant was mixed with inhibitor at indicated concentration in the buffer containing 50 mM MOPS pH 7.4, 0.05 mM CHAPS, 50 mM NaF and 0.1 mg/mL BSA, and incubated for 15 min at room temperature. After adding 7.5 μg/mL Nickerl chelate beads,7.5 μg/mL Streptavidin beads and 200 nM His-BCOR, the mixture was then incubated for additional 1.5 hrs at 20 ℃. Finally, the mixture was transferred to 384-well plate and analyzed by a EnVision 2105 (PerkinElmer).

Biolayer Interferometry Assay (BLI)

Bio-layer interferometry equipment (Gator Bio) was used to determine the binding affinity between iBP and the PCGF1^{RAWUL} L238A/F242A mutant. Biotinylated PCGF1^{RAWUL} L238A/F242A at concentration of 50 μg/mL was immobilized on a SA XT biosensor. To remove non-specific bound, the biosensors were washed with assay buffer (50 mM MOPS pH 7.4, 0.05 mM CHAPS, 50 mM NaF, 0.1 mg/mL BSA and 0.5% DMSO). After obtaining a baseline reading in assay buffer, the biosensors were dipped into reference well or wells containing the various concentration of iBP for 5 min. Then, the biosensors were washed with assay buffer for 2 min. Binding kinetics were analyzed using 1:1 binding model with on-board software. Data were plotted using GraphPad Prism software.

Scanning electron microscope (SEM) and transmission electron microscopy (TEM)

The surface structure of the F127 hydrogel (20% W/V) was examined using SEM. Samples were freeze-dried using an LGJ-12A freeze dryer (China), gold-coated, and imaged with a Zeiss Gemini 300 SEM. The morphology of iBP was observed under a HT7700 TEM (Hitachi High-Tech, Tokyo, Japan). The size and size distribution of

iBP particles were further analyzed using a Zetasizer Nano ZS automatic particle size detector (Malvern, UK).

***In vitro* drug release assay**

The release profile of iBP from the F127 hydrogel-gelatin sponge was assessed using a dialysis membrane with a molecular weight cut-off (MWCO) of 3500 Da. Sponges loaded with either 2 mg/mL (100 μL) or 4 mg/mL (100 μL) of iBP (measuring 2x2x10 mm3) were placed in 100 mL of PBS at 37°C with continuous stirring at 100 rpm. At each time point, 1 mL of the solution was removed and replaced with 1 mL of PBS to maintain a constant volume. The concentration of iBP in the solution was determined using a standard curve established at OD_{300} nm, recorded with a U-3310 spectrophotometer (Hitachi High-Tech, Tokyo, Japan).

Supplementary Figures

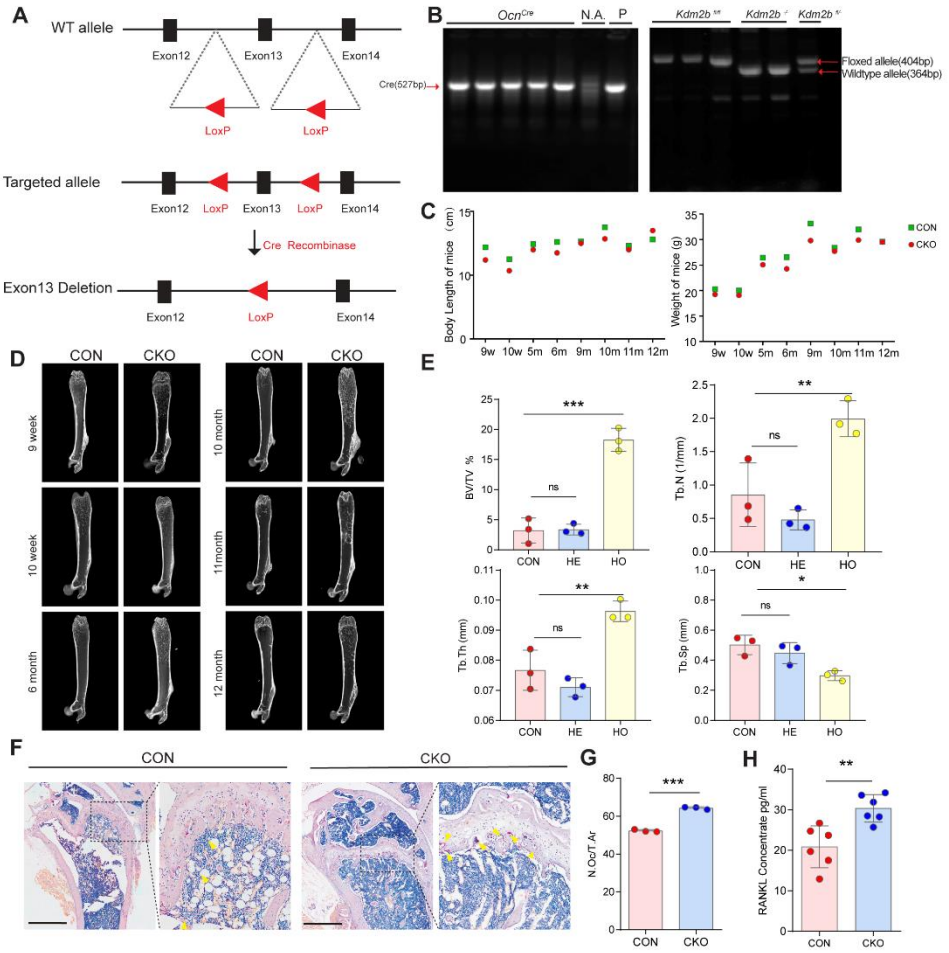

Fig S1. Selective ablation and phenotypic characterization of the KDM2B-CxxC in femur.

(A) Schematic representation of the *Kdm2b* genomic structure (top), targeting allele (middle) and targeted allele (bottom). Exon 13 is flanked by two *loxP* sites and will be excised after mating with Cre-recombinase-expressing mice. **(B)** PCR products for respective genotypes. **(C-D)** Representative images of scanning coronal sections of femurs and statistical analysis of body weight (C) and images (D) of femur of *Kdm2b*$^{fl/fl}$ *Ocn*^{Cre} mice at different ages. **(E)** μCT analysis of trabecular parameters (n=3 mice per genotype). Statistical tests were performed using ordinary one-way ANOVA for (E), * $P < 0.05$, ** $P < 0.01$, *** $P < 0.001$. **(F-G)** Images of TRAP staining of femurs from *Kdm2b*$^{fl/fl}$ *Ocn*^{Cre} mice and controls, box areas shown at a higher magnification to the right (F). TRAP-positive OCs marked with yellow triangles. Statistical analysis of number of OCs of femurs from *Kdm2b*$^{fl/fl}$ *Ocn*^{Cre} mice and controls (G) (n = 3 mice per genotype). **(H)** The concentration of RANKL in serum was detected by ELISA (n=6). Statistical tests were performed using Student's *t* tests for (G) and (H). *$P < 0.05$, **$P < 0.01$, ***$P < 0.001$, ns, not significant., CON: (*Ocn*^{Cre} mice), HE: Heterozygote (*Kdm2b*$^{fl/-}$ *Ocn*^{Cre} mice), HO: Homozygote (*Kdm2b*$^{fl/fl}$ *Ocn*^{Cre} mice).

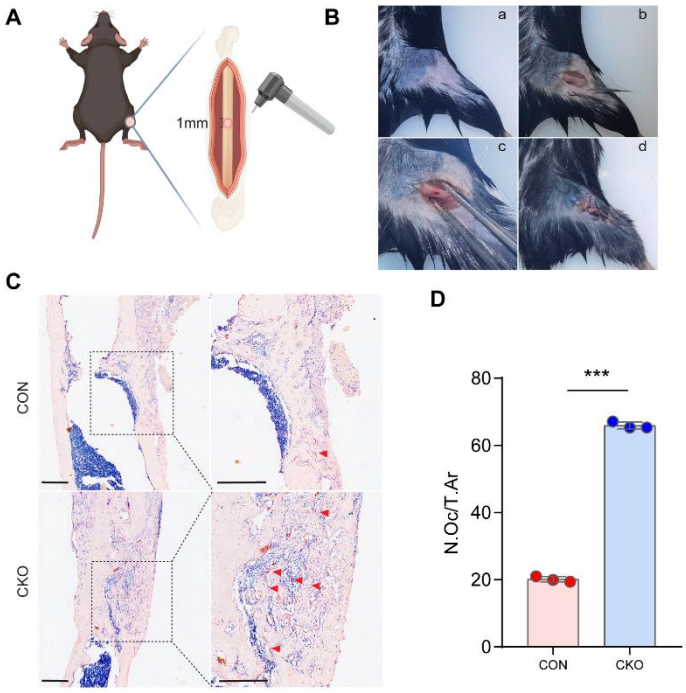

Fig S2. Construction of bone defect model.

(A) Schematic diagram of preparation of a 1 mm diameter circular defect located in the middle of the femur. **(B)** Process of bone defect preparation: a, shaving right lower limb; b, exposing the right femur; c, preparing circular defects; d, postoperative suture. **(C)** Representative images of TRAP staining in the bone defect area from *Kdm2b*$^{fl/fl}$ *Ocn*^{Cre} mice and controls, with box areas shown at a higher magnification to the below. TRAP-positive OCs are indicated by yellow triangles. (**D**) Quantitative analysis of OC numbers in the newly formed bone within the bone defect area for each genotype (n=3 mice per genotype). Statistical significance was determined using Student's *t* tests, ***$P < 0.001$.

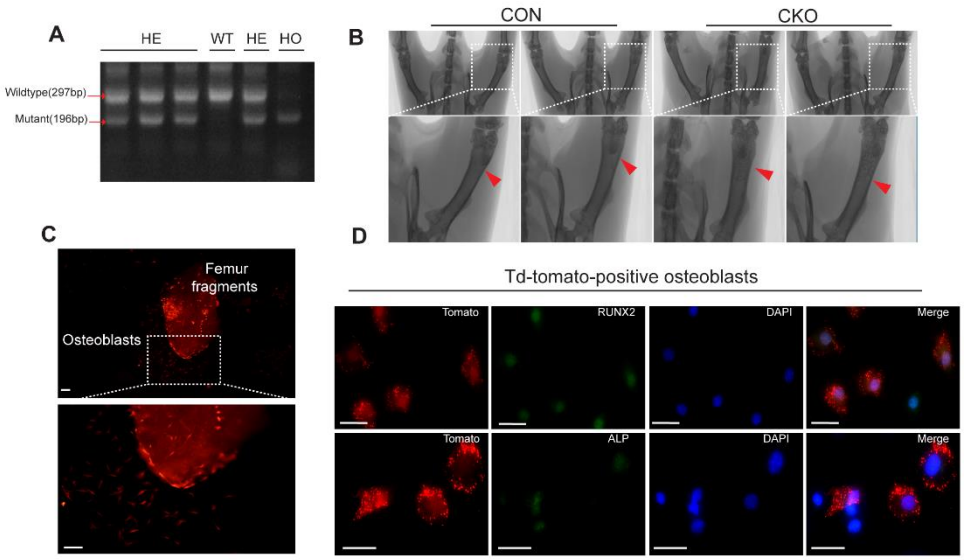

Fig S3. Screening of tomato-positive osteoblasts from *Kdm2b*$^{fl/fl}$*Ocn*^{Cre} *td-Tomato* mice.

(A) PCR products for each genotype. **(B)** μCT analysis of right lower limb of live mice, with trabecular marked with red triangles. **(C)** Fluorescence microscopy images depicting tomato-positive cells emerging from cultured bone fragments, with the boxed areas shown at a higher magnification to the below. **(D)** IF images of osteogenesis-related marker proteins (RUNX2/ALP) in tomato-positive OBts. WT: wildtype of *td-Tomato* mice, HE: Heterozygote of *td-Tomato* mice, HO: Homozygote of *td-Tomato* mice.

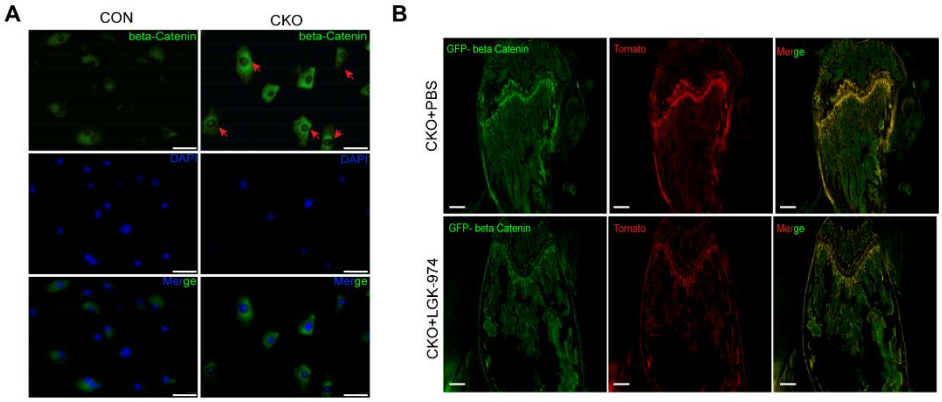

Fig S4. KDM2B inactivation enhances OB functions through the activation Wnt/β-catenin signaling

(A) Representative IF images showing β-Catenin localization in tomato-positive osteoblasts isolated from CON and CKO mice. Red arrows indicate β-Catenin translocation to the nucleus. **(B)** Representative IF images representing β-Catenin staining in the femur metaphysis of CKO mice, with or without LGK974 treatment for 1 mon. CON: *Ocn*^{Cre} *tdTomato* mice, CKO: *Kdm2b*$^{fl/fl}$ *Ocn*^{Cre} *tdTomato* mice

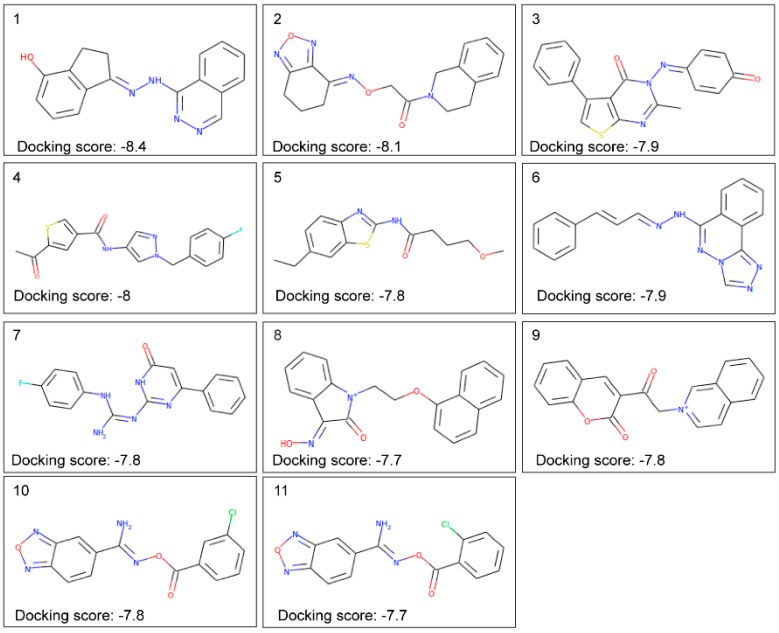

Fig S5. Screening of inhibitors targeting PRC1.1 by blocking interaction of BCOR-PCGF1.

Chemical molecular formulas and docking scores of selected candidate inhibitors (1-11).

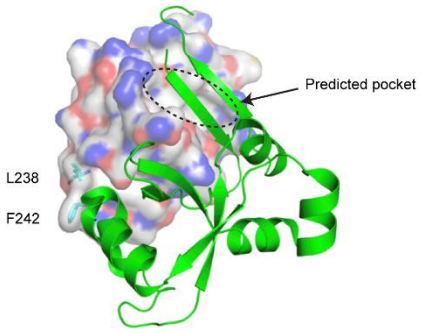

Fig S6. Crystal structure of PCGF1^{RAWUL}-BCOR^{PUFD} complex (PDB:4HPL)
The L238 and F242 residues on PCGF1 are shown as cyan sticks. RAWUL domain of PCGF1 is shown as surface (white for carbon, red for oxygen, blue for nitrogen, and yellow for sulfur). PUFD domain of BOCR is shown as green cartoon.

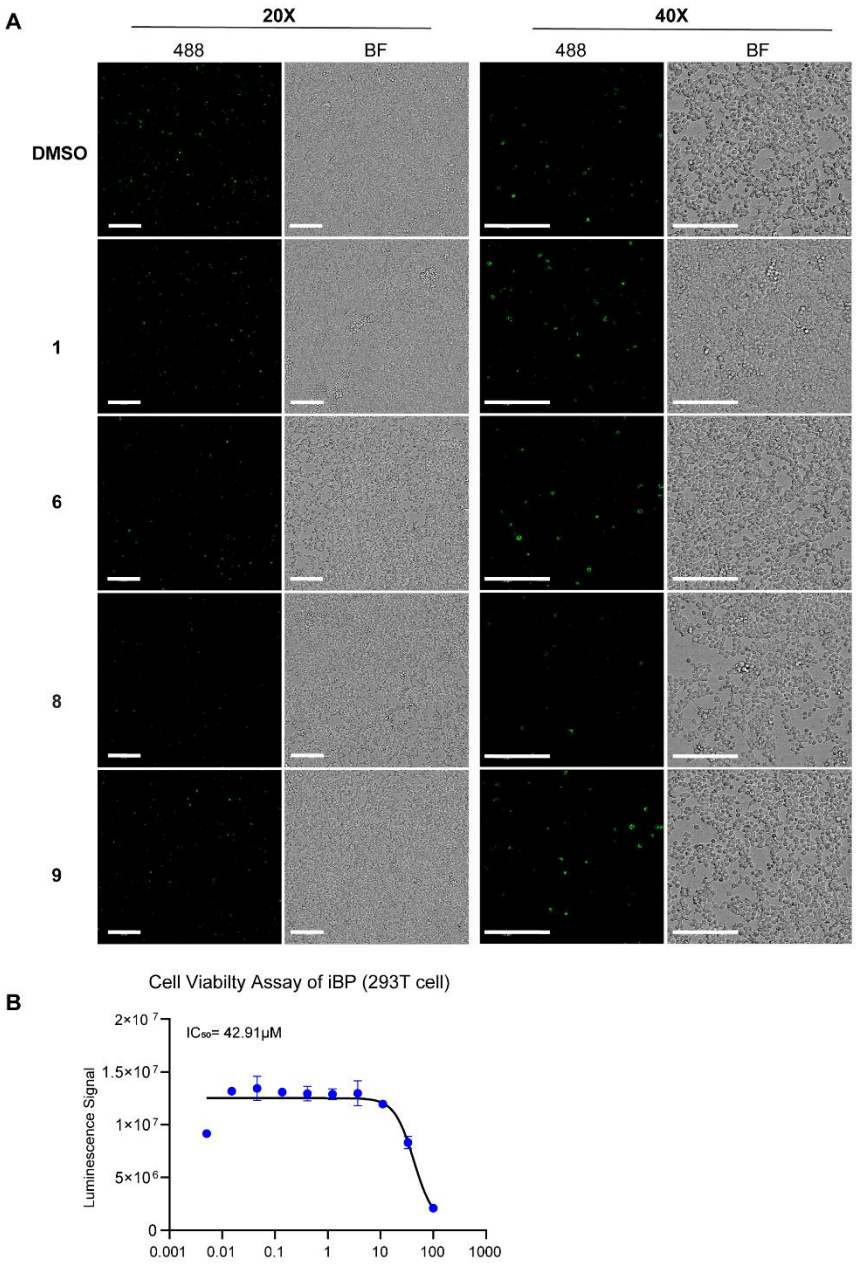

Fig S7. Inhibition efficiency and cell viability assay of candidate compounds. **(A)** Representative Images from high-content screening system showing GFP expression in 293T cells co-transfected with plasmids GFP1-10-PCGF1 and GFP11-BCOR, following treatment with candidate inhibitors after 48 hrs of culture. **(B)** Determination of the IC_{50} of iBP in 293T cell using a Cell Viability Assay kit.

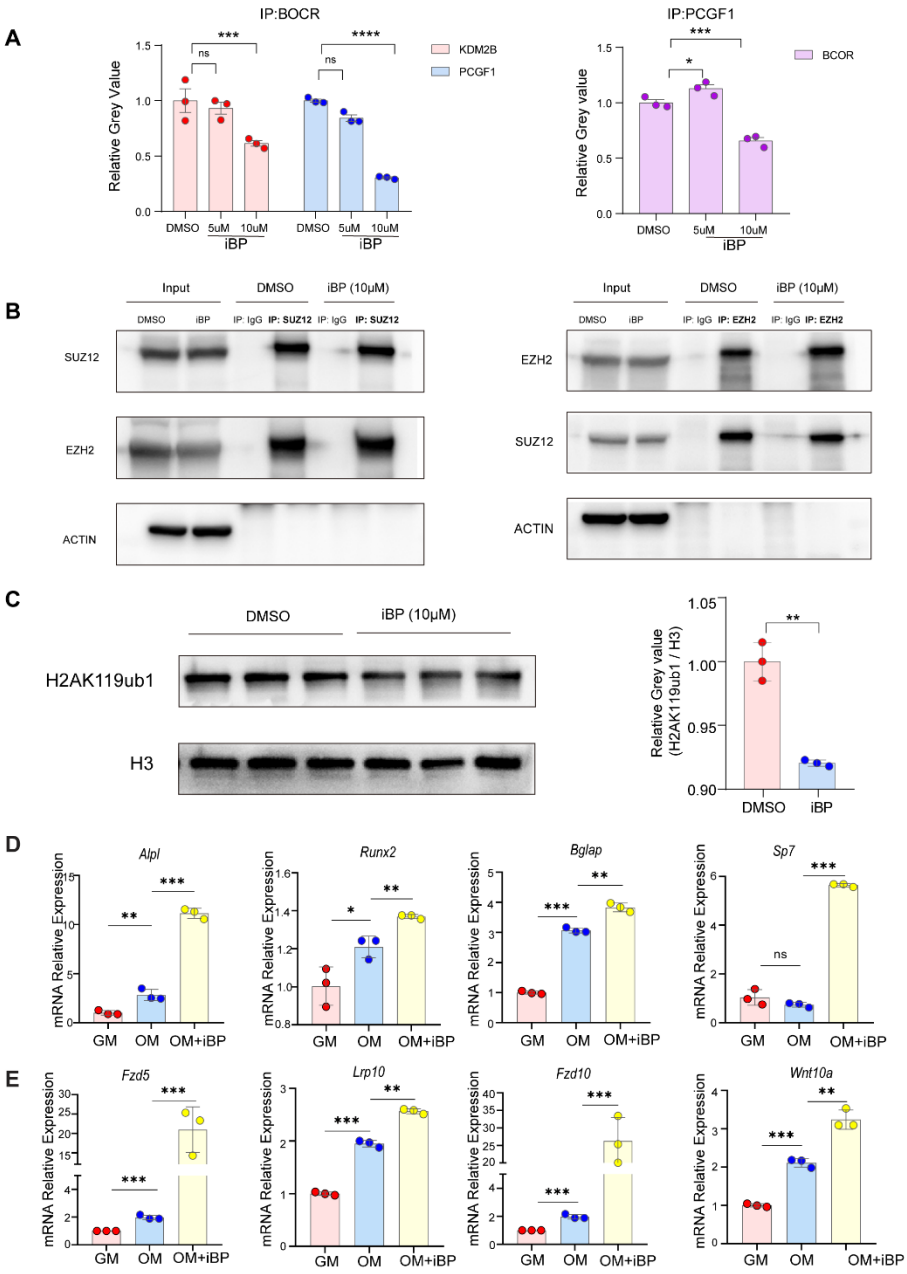

Fig S8. Biochemical and functional Characterization of iBP in cells.

(A) Statistical analysis of gray values of Fig 6, I and J. (**B**) Co-IP assay showing the unaltered interaction between SUZ12 and EZH2. (**C**) WB assay showing the reduction of global H2AK119ub levels following iBP treatment. Quantification of the normalized H2AK119ub1 levels was conducted, and statistical significance was assessed using Student's *t* tests, $^{**}P < 0.01$. **(D-E)** RT-qPCR analysis of leading genes of the Wnt pathway and osteogenesis-related genes in 3T3-E1 cells cultured with osteogenic medium for 7 days in the presence or absence of iBP treatment. Statistical tests were performed using ordinary one-way ANOVA for (A), (D) and (E), $^{*}P < 0.05$, $^{**}P < 0.01$, $^{***}P < 0.001$, $^{****}P$ value < 0.0001, ns, not significant.

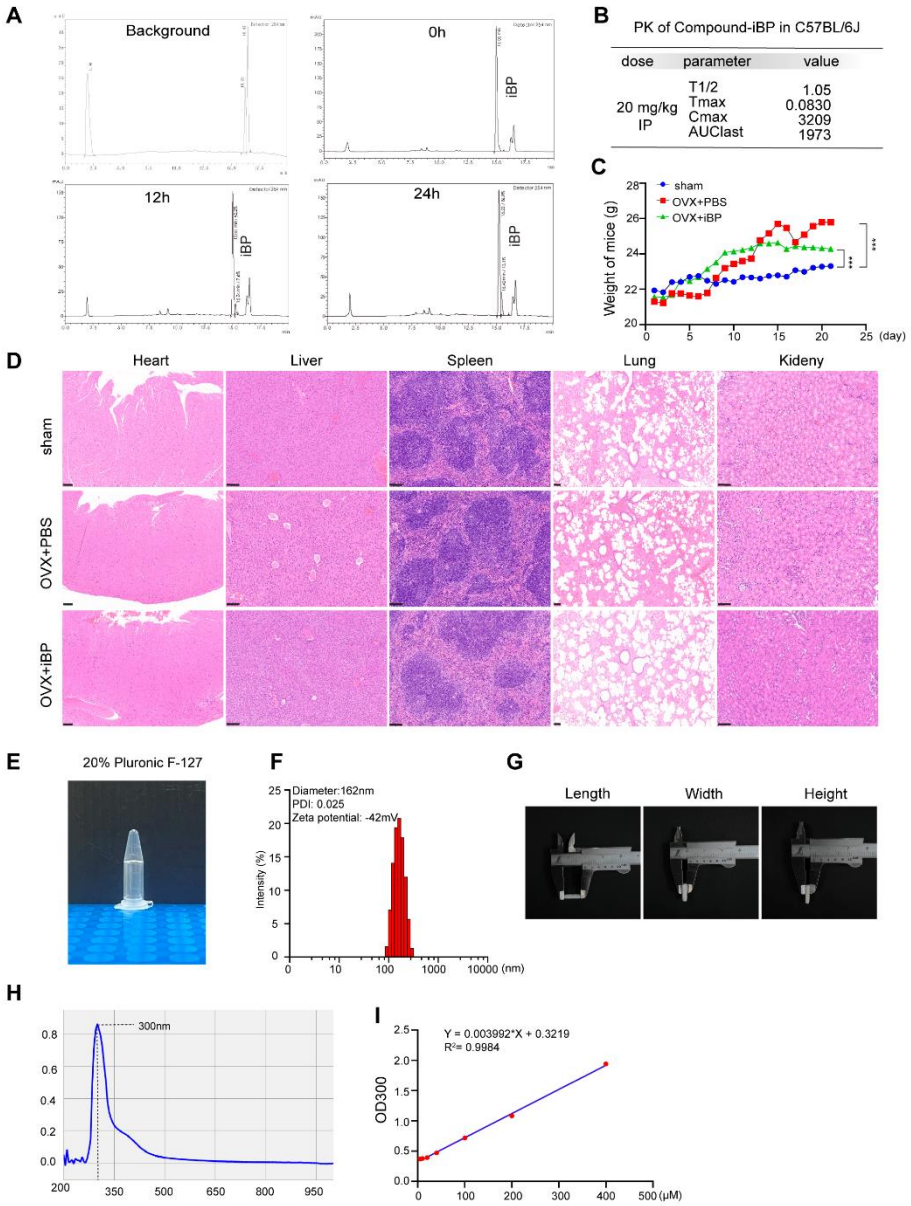

Fig S9. Characterization and systemic administration of iBP.

(A) HPLC analysis of iBP stability in serum medium at 12 and 24 hrs. **(B)** Pharmacokinetic profile of iBP. **(C)** Statistical analysis of weight of setting-up groups (n=5 mice per group). Statistical significance was assessed using ordinary one-way ANOVA, ***P<0.001. **(D)** Representative images of HE staining of heart, liver, spleen, lung and kidney from each group. **(E)** Visual representation of F127 hydrogel at 30% concentration at room temperature. **(F)** Particle size distribution analysis of iBP nanoparticles. **(G)** Measurement of the dimensions (length, width, and height) of the gelatin sponge used in the study. **(H)** Ultraviolet visible absorption spectrum analysis of iBP. **(I)** Standard curve of iBP (OD= 300 nm).

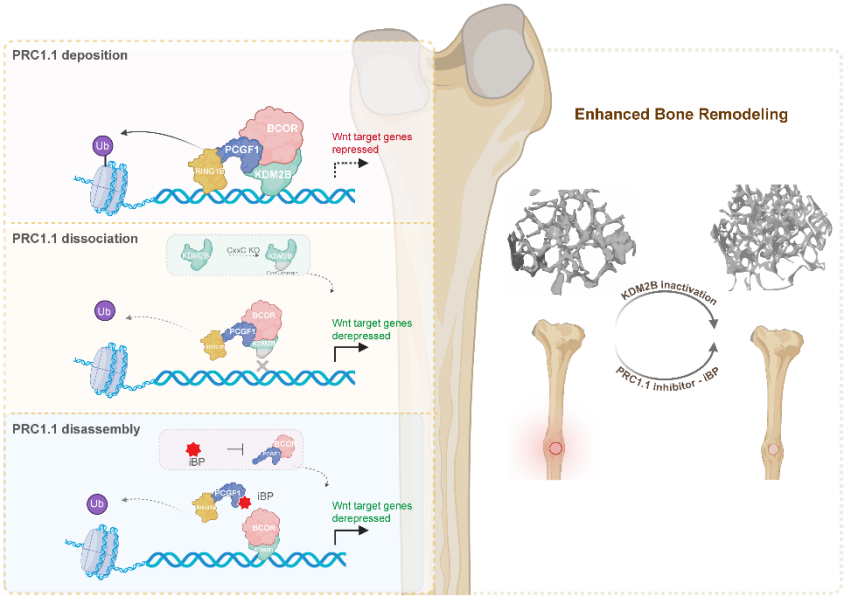

Fig. S10. Working model of this study

Deletion of the KDM2B-CxxC domain leads to PRC1.1 dissociation, enhancing bone remodeling through Wnt signaling activation and associated loss of H2AK119ub1 at target genes. Similarly, PRC1.1 inhibition via complex disassembly by a small-molecule inhibitor counteracts bone loss in pathological conditions, including osteoporosis and acute trauma.